

Understanding Hydrodynamics in the Western Scheldt Estuary

Sarah Brannum

December 7th, 2024

Abstract

The Western Scheldt estuary has dynamic sediment and water transport that has implications for coastal resiliency. Using a Delft3D hydro-morphodynamic simulation, time-varying water levels and velocity throughout the estuary were calculated over 3 days. The deepest regions of the estuaries correlate to the dredging channels for navigation. The velocities are highest in the dredging channels, which enter and exit the estuary during the high and low tide transitions. The tidal range becomes amplified moving landward in the estuary, peaking at over 3 m in the inner regions. The high and low tide velocities differ, indicating tidal asymmetry within the system.

1 Introduction

Coastal environments are hydrodynamically complex due to interactions between terrestrial and oceanic water forces and fluxes (9). It is imperative to understand coastal hydrodynamics due to flood risk, navigation, ecosystem resiliency, and coastal infrastructure (1). Both Louisiana and the Netherlands are areas that built infrastructure on deltaic floodplains. Deltaic floodplains exist by major rivers depositing sediment along the coast that eventually becomes subaerial land. Both places utilize a complex series of levees, both natural and artificial, to support communities and economic activity from their respective ports. Human modification of coastal environments is necessary to protect from flood damage and best utilize the land. However, natural sediment and water movements can directly counteract these efforts; human infrastructure seeks to reduce variability and extremes that natural systems are prone to.

The Western Scheldt is one of the best modeled and understood estuaries in the world due to the importance of trade and proximity to premier Dutch research institutions (3). The Western Scheldt estuary is the outlet for the port of Antwerp in Belgium, where millions of dollars of goods are exchanged each year. The large cargo ships need deeper channels, so regular dredging occurs through specific passages (3). Without dredging, the channels would infill with sediment due to suspended sediment carried from the river and resuspended

from the bed (6). The stability of the bed required for navigation directly opposes the natural dynamic environment of estuaries, driving the need for human intervention. The Western Scheldt is not only dredged, but contains levees and dams that keep water within certain regions and ensures flood protection for the land surrounding the estuary (6).

To understand how to mitigate flood damage in the Western Scheldt, it is vital to understand the processes that dictate change and the hydrodynamics of the system. The purpose in this project is to explore changes in the different variables that drive water movements. Using a Delft3D hydro-morphodynamic simulation, I aim to do the following tasks:

1. Explore variables that Delft3D provides
2. Plot elevation of the domain
3. Plot water velocity throughout the simulation
4. Plot water height throughout the simulation

By creating figures, important details about the hydrodynamics of the Western Scheldt can be ascertained.

2 Methods

Delft3D is the hydro-morphodynamic numerical model used in this study (Deltares). It conserves water mass and momentum across adjacent grid cells at each time step by solving a series of differential equations (7). This model is an unstructured grid with more than 36 million grid cells within the Western Scheldt estuary (Figure 2). Certain areas of the domain are more refined than others, which saves computational time by using larger grid cells in areas that are not as dynamic.

The time steps ranged from 1 to 30 seconds according to the location and time within the simulation. The simulation ran for 3 days total, and saved output data in 1 hour increments for a total of 72 time files of output information.

I used various Python packages to plot the output results. The output file from a Delft3D simulation is netcdf. The primary package I used was Deltares/dfm_tools, which contains python code about the file structures and how to plot the output data (Veenstra). I also used matplotlib.pyplot to make aesthetically pleasing figures, xarray and pandas to manipulate the netcdf, and numpy to perform computations on the arrays.

First, I created a pandas array that lists all of the variables that the netcdf contains. Delft3D provides information on variables such as water level, velocity, shear, stress, bed level, and many others at each grid cell for each time step. I saved the pandas array as a .csv file, which I read into Microsoft Excel to have a resource of the variables and their stored names to refer to.

Using information about the variables available, I created various plots to convey changes in these variables over time. I plotted the grid itself, with a

background of the OpenStreetMap of the surrounding area (Figure 2). I also plotted the initial bathymetry, or depth of the domain at every grid cell (Figure 3).

Next, using the velocity in the u and v directions of each cell, I converted the velocity into a magnitude and direction (Figures 4 and 5). The quiver plot has arrows that correspond to the magnitude and the direction of the water velocity.

3 Results

standard_name	units	location	shape	dimensions	dtype	long_name
			[0]	[]	int32	
			[0]	[]	int32	Topology data of 2D mesh
projection_x_coordinate	m		(6235,)	('mesh2d_nNodes',)	float64	x-coordinate of mesh nodes
projection_y_coordinate	m		(6235,)	('mesh2d_nNodes',)	float64	y-coordinate of mesh nodes
altitude	m	node	(6235,)	('mesh2d_nNodes',)	float64	z-coordinate of mesh nodes
projection_x_coordinate	m		(12362,)	('mesh2d_nEdges',)	float64	Characteristic x-coordinate of the mesh edge (e.g. midpoint)
projection_y_coordinate	m		(12362,)	('mesh2d_nEdges',)	float64	Characteristic y-coordinate of the mesh edge (e.g. midpoint)
			(12362, 2)	('mesh2d_nEdges', 'Two')	int32	Start and end nodes of mesh edges
			(6078, 4)	('mesh2d_nFaces', 'mesh2d_nMax_face_nodes')	float64	Vertex nodes of mesh faces (counterclockwise)
			(12362, 2)	('mesh2d_nEdges', 'Two')	float64	Neighboring faces of mesh edges
projection_x_coordinate	m		(6078,)	('mesh2d_nFaces',)	float64	Characteristic x-coordinate of mesh face
projection_y_coordinate	m		(6078,)	('mesh2d_nFaces',)	float64	Characteristic y-coordinate of mesh face
projection_z_coordinate	m		(6078, 4)	('mesh2d_nFaces', 'mesh2d_nMax_face_nodes')	float64	x-coordinate bounds of mesh faces (i.e. corner coordinates)
projection_y_coordinate	m		(6078, 4)	('mesh2d_nFaces', 'mesh2d_nMax_face_nodes')	float64	y-coordinate bounds of mesh faces (i.e. corner coordinates)
cell_area	m ²	edge	(12362,)	('mesh2d_nEdges',)	float64	edge type (relation between edge and flow geometry)
cell_area	m ²	face	(6078,)	('mesh2d_nFaces',)	float64	
altitude	m	face	(6078,)	('mesh2d_nFaces',)	float64	flow element center bedlevel (b)
time			(73,)	('time',)	datetime64[ns]	
	s		(73,)	('time',)	float64	Latest computational timestep size in each output interval
	1 face		(73, 6078)	('time', 'mesh2d_nFaces')	float64	Number of times flow element was Courant limiting
sea_surface_height	m	face	(73, 6078)	('time', 'mesh2d_nFaces')	float64	Water level
sea_surface_height	m	face	(73, 6078)	('time', 'mesh2d_nFaces')	float64	Water level on previous timestep
sea_floor_depth_below_sea_surface	m	face	(73, 6078)	('time', 'mesh2d_nFaces')	float64	Water depth at pressure points
	ms-1	edge	(73, 12362)	('time', 'mesh2d_nEdges')	float64	Velocity at velocity point, n-component
	ms-1	edge	(73, 12362)	('time', 'mesh2d_nEdges')	float64	Velocity at velocity point at previous time step, n-component
sea_water_x_velocity	ms-1	face	(73, 6078)	('time', 'mesh2d_nFaces')	float64	Flow element center velocity vector, x-component
sea_water_y_velocity	ms-1	face	(73, 6078)	('time', 'mesh2d_nFaces')	float64	Flow element center velocity vector, y-component
sea_water_speed	ms-1	face	(73, 6078)	('time', 'mesh2d_nFaces')	float64	Flow element center velocity magnitude

Figure 1: Abbreviated table of the different variables in the netcdf output file with information about how they are stores, units, and other metadata

By creating a table, it is easier to see the different variables and associated metadata with each (Table 1). The output variables are either stored on the grid cell, grid edge (grid line) or node (intersection between grid line).

The domain specifically isolates areas within the estuary by taking advantage of the unstructured grid option in Delft3D (Figure 2). The deepest parts of the Western Scheldt correspond to the dredged channel (Figure 3). The depth toward the ocean increases uniformly across the domain (Figure 3). The deepest depth in the domain is 46.89 m below MSL, while the highest elevation is 3.54 m above MSL.

The quiver plots (figures 4 and 5) show the velocity across the domain 6 hours apart. The Western Scheldt has semi-diurnal tides with 2 high tides and 2 low tides each day. Figure 4 shows the tides entering the estuary with the highest velocities, while figure 5 shows the tide leaving the estuary with the highest velocities. Comparing the velocity at high and low tide specifically show differences in their magnitudes (Figures 6c and 6d). The largest velocity difference is located in the shallow regions compared to the channel (Figure 7).

I compared the water height at the high and low tide (Figures 6a and 6b).

The higher water heights are at high tide, while the lower water heights are during low tide. The highest differences in water height are located within the estuary itself, specifically the uppermost reaches (Figure 8). The tidal range can exceed 3 meters in the upper reaches. In the oceanic side of the domain, the water height difference between high and low tide is very close to zero, indicating limited vertical movement in water due to the tide.

For each result, I created figures with high resolution (600 dpi) and large fonts that are appropriate for presentations. I also created a gif of the water level and velocity magnitudes over the simulation duration. I used Davinci Resolve in order to take the images and export as a single video while maintaining proper video quality. I appropriately scaled each figure to the maximum and minimum values in the dataset, and used colorbar schemes appropriate with the variable at hand.

4 Discussion

Tidal asymmetry refers to the difference in water velocity between the ebb and flood tides (3). Tidal asymmetry has important ramifications for estuarine dynamics by impacting sediment retention in the estuary from the ocean versus terrestrial sources. A higher flood tidal velocity can cause more oceanic sediments to stay within the estuary, while a higher ebb tidal velocity can cause terrestrial sediments to stay within the estuary. A tidal asymmetry can create an ebb or flood tidal delta, a deposit of sediment at the mouth of the estuary. This deposit can cause navigation concerns, which would lead to the need for more dredging. Hydrodynamically, high ebb tidal velocities can flush anthropogenic pollutants from the land out of the system.

Although there are different hydrodynamic forcings in the simulation including waves and rivers, the periodic water height fluctuations can be attributed to the tides because of the uniform time change. The highest water heights and lowest are offset by 6 hours, and repeat every 12 hours. This time signature is consistent with semi-diurnal tides, which is the prominent tidal period in the Western Scheldt (3).

Tidal amplification is evident by the spatial difference in tidal height across the domain. Tidal amplification has ramifications for coastal protection by causing higher water levels in areas deeper in the estuary. Storms off the coast can bring high waves, which can be amplified by the tidal amplification of the Western Scheldt (6). Landward communities and infrastructure, particularly connected to the port of Antwerp, are particularly vulnerable to flood damage because of tidal amplification. Tidal amplification also necessitates deeper dredged channels because the vessels require deep enough channels at all times of day, including when water levels are 3 meters shallower at low tide.

Coastal Louisiana experiences the same dynamic environment as the Western Scheldt with key differences that impact coastal resiliency. Both are low-lying regions with valuable economic activity for their respective countries. Louisiana boasts the port of New Orleans with access to the U.S.'s extensive riverine in-

land trading network. Conversely, the port of Antwerp is one of the largest ports in Belgium. Louisiana is vulnerable to tropical storms, which can bring surges upward of 5 meters and winds over 70 m/s. The added risk in Louisiana requires more robust infrastructure to protect communities and economic output. Both ecosystems have various marsh grass species, with the Western Scheldt boasting saltwater marsh species while Louisiana marshes are majority freshwater. Both coastlines are heavily anthropogenically modified by dredging and levee building. Louisiana is a river-dominated delta, while the Western Scheldt is a tidal-dominated delta.

A key difference is the active land building that is occurring in Louisiana. Louisiana had expansive deltaic wetlands that facilitate sediment deposition out of the Mississippi River. However, Louisiana has been losing land along the coast due to saltwater intrusion killing vegetation that facilitate sediment deposition, reduced sediment supply from the river, and high local sea level rise rates (2). Coastal land loss is a concern for all coastlines due to eustatic sea level rise due to climate change, which will also threaten land adjacent to the Western Scheldt (2).

While both systems are heavily engineered, each region has a different approach to protecting their coastline. The Netherlands primarily builds hard engineering structures that directly protect against high water levels. By fortifying infrastructure at the government level, the country can be protected. Meanwhile, southern Louisiana takes advantage of the natural system by employing nature based solutions. The Coastal Master Plan outlines efforts to restore vegetation and facilitate sediment deposition to combat land loss (4). Additionally, sediment diversions are man-made versions of crevasse splays that create subaerial land from natural river avulsions (8). Effective coastal protection is a result of both nature-based and engineering solutions.

Python is a valuable tool to format, manipulate, and plot Delft3D output because of the extensive packages and straightforward code. Having a plethora of online packages created by other people provides resources to help create figures. Additionally, reading netcdf files is greatly simplified by the use of the xarray package, which also allows users to easily determine which variables are included in the file as well as helpful metadata to understand the output.

5 Conclusion

In summary, the Western Scheldt is hydrodynamically complex despite only looking at water level and velocity for the purposes of this study. It is important to understand hydro-morphodynamics in the region for coastal management, flood risk, ecosystem resiliency, and economic value. A Delft3D simulation of the Western Scheldt calculated water level and velocity throughout the course of the simulation duration. The semi-diurnal tides were evident by the 6 hour time-delay between high and low tide. The velocity of the water is highest during the transition between high and low tide. The difference in magnitude of the high and low tide velocity is due to a tidal asymmetry. The high tide experiences

the highest water height, while low tide experiences the lowest water height throughout the entire domain. However, the spatial variation in tidal range is due to tidal amplification, where inland areas of the estuary have higher tidal heights compared to the oceanic regions where tidal range is negligible. Python is an effective way to create, manipulate, and plot complex datasets from model outputs, specifically Delft3D.

References

- [1] Barbier, E. B. (2019). The value of coastal wetland ecosystem services. In *Coastal wetlands*, pages 947–964. Elsevier.
- [2] Blum, M. D. and Roberts, H. H. (2009). Drowning of the mississippi delta due to insufficient sediment supply and global sea-level rise. *Nature geoscience*, 2(7):488–491.
- [3] Bolle, A., Wang, Z. B., Amos, C., and De Ronde, J. (2010). The influence of changes in tidal asymmetry on residual sediment transport in the western scheldt. *Continental Shelf Research*, 30(8):871–882.
- [4] CPRA (2023). *2023 Louisiana Coastal Master Plan*. Coastal Protection and Restoration Authority.
- [Deltaires] Deltaires. Deltaires-usa.
- [6] Elias, E. P., Van der Spek, A. J., Wang, Z. B., Cleveringa, J., Jeuken, C. J., Taal, M., and Van der Werf, J. J. (2023). Large-scale morphological changes and sediment budget of the western scheldt estuary 1955–2020: the impact of large-scale sediment management. *Netherlands Journal of Geosciences*, 102:e12.
- [7] Lesser, G. R., Roelvink, J. v., van Kester, J. T. M., and Stelling, G. (2004). Development and validation of a three-dimensional morphological model. *Coastal engineering*, 51(8-9):883–915.
- [8] Nienhuis, J. H., Törnqvist, T. E., and Esposito, C. R. (2018). Crevasse splays versus avulsions: A recipe for land building with levee breaches. *Geophysical Research Letters*, 45(9):4058–4067.
- [9] Ribas, F., Falques, A., De Swart, H. E., Dodd, N., Garnier, R., and Calvete, D. (2015). Understanding coastal morphodynamic patterns from depth-averaged sediment concentration. *Reviews of Geophysics*, 53(2):362–410.
- [Veenstra] Veenstra, J. dfm_tools: A Python package for pre- and postprocessing D-FlowFM model input and output files.

6 Figures

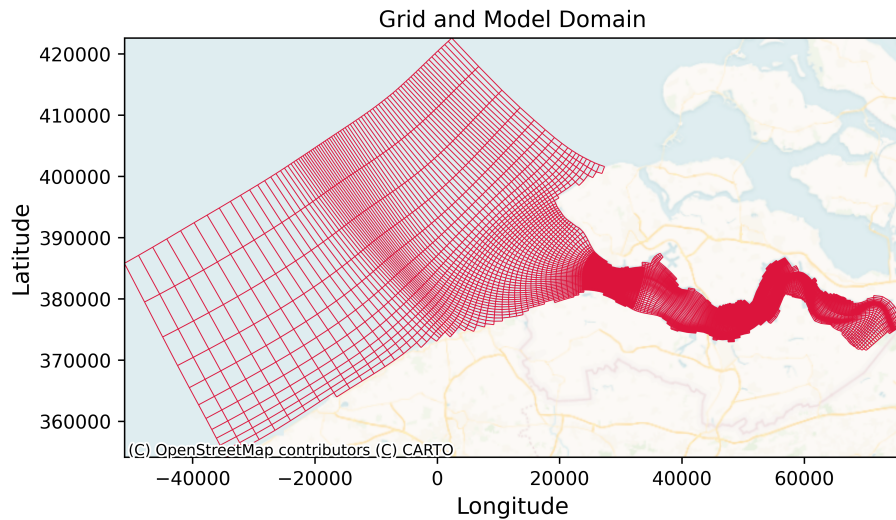


Figure 2: Grid and Model domain of the Western Scheldt Estuary

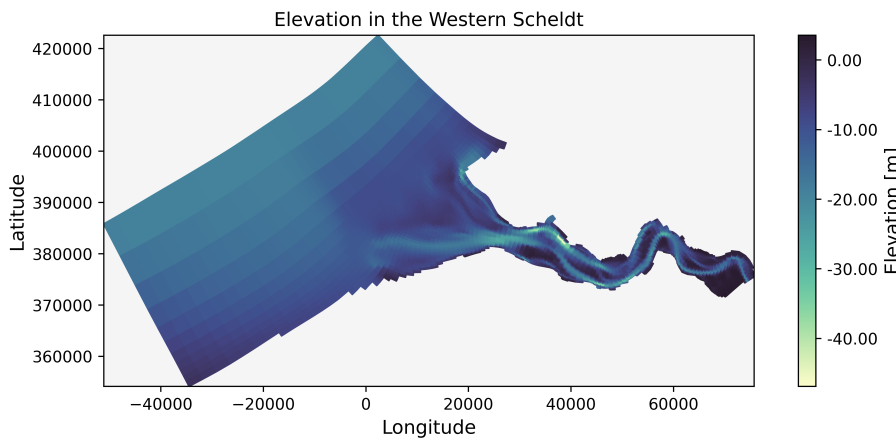


Figure 3: Bathymetry of the Western Scheldt Estuary

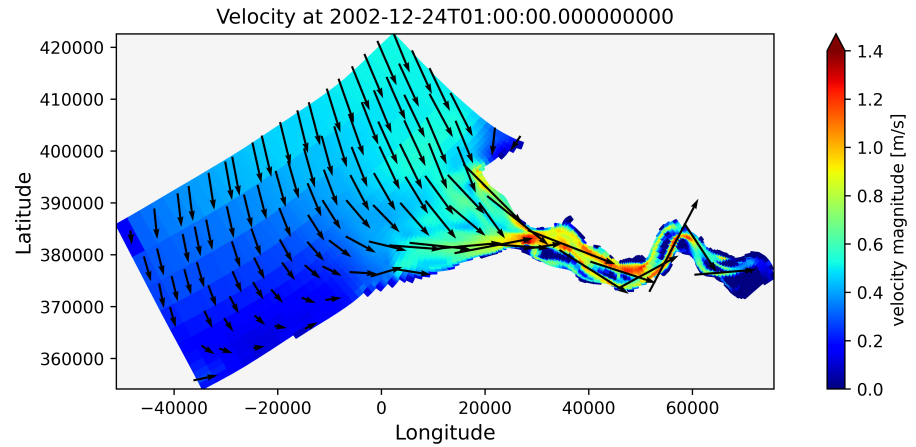


Figure 4: Velocity as the tide comes into the estuary

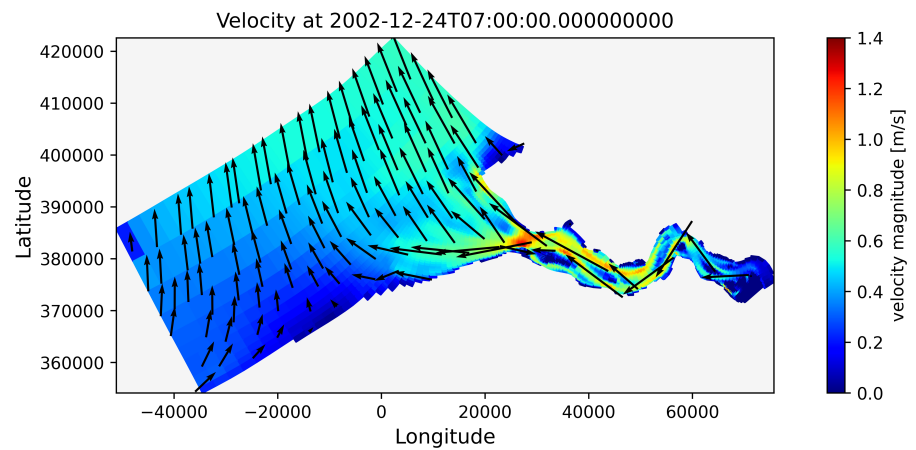


Figure 5: Velocity as the tide leaves the estuary

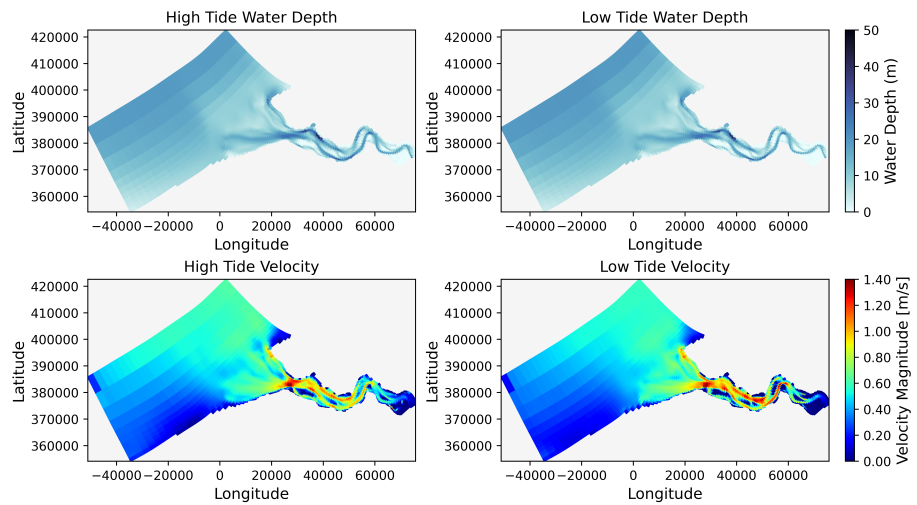


Figure 6: Water height and velocity magnitude at high and low tide

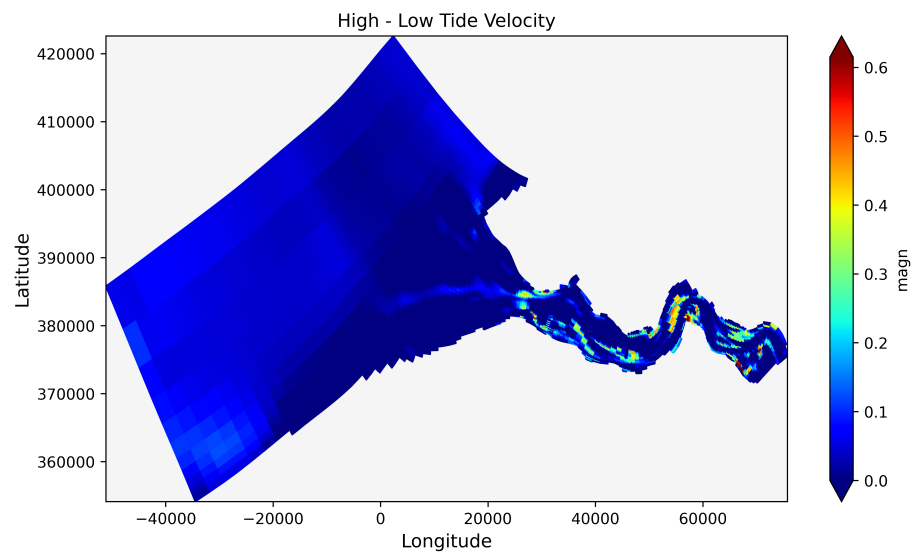


Figure 7: Difference in velocity magnitude between high and low tide

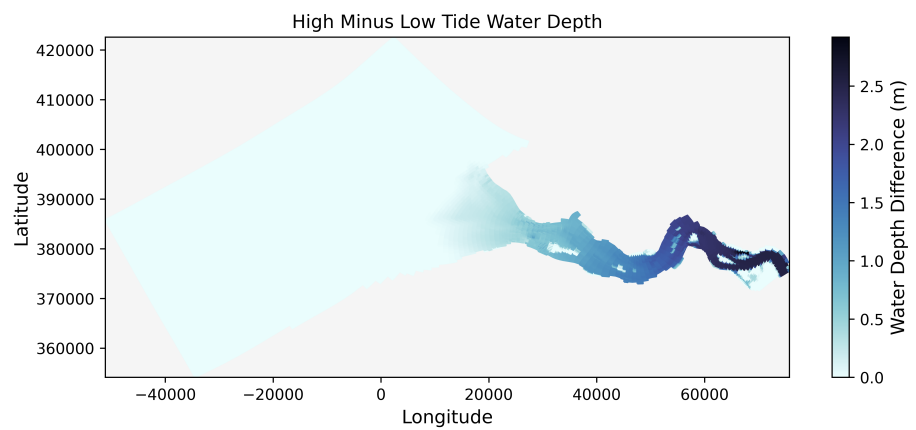


Figure 8: Difference in water height at high and low tide